Desalination and Water Treatment
www.deswater.com

doi:10.5004/dwt.2017.20202

66 (2017) 88–96
March

An unusual datura pod structure for calcite—Effect of EGTA on the morphology and polymorphism of $CaCO_3$

S. Bhuvaneswari[a,b], K. Palanisamy[c], K. Subramani[a,d], V.K. Subramanian[c,*]

[a]*R&D Center, Bharathiyar University, Coimbatore. Tamil Nadu, 641046, India*
[b]*Dept. of Chemistry. Govt. Arts College, Tindivanam, Tamil Nadu, 604 001, India*
[c]*Department of Chemistry, Annamalai University, Annamalainagar, Tamil Nadu 608002, India. Tel. +91 94862 82324*
email: drvksau@gmail.com (V.K. Subramanian)
[d]*Department of Chemistry, Islamaiya College, Vaniambadi, Tamil Nadu, 635752, India*

Received 14 May 2016; Accepted 27 August 2016

ABSTRACT

Scale formation is a serious problem often observed in heat transfer equipments. Barite, calcite and aragonite are some of the major components of scale. Control of scale formation is usually achieved through usage of scale inhibitors/chelating agents. Here we report the effect of ethylene glycol-O,O′-bis(2-aminoethyl)-N,N,N′,N′-tetraacetic acid (EGTA) on the morphology and polymorphism of $CaCO_3$ when synthesized from $CaCl_2$ solution using Na_2CO_3 at three different temperatures, 60, 80 and 100°C. The samples were characterized using XRD, FTIR and SEM techniques. The details revealed that EGTA stabilizes aragonite more efficiently at 60°C and with raise in temperature formation of calcite is predominant. The study revealed an unusual and novel datura pod like morphology for calcite.

Keywords: Scale; Crystal growth; Calcite; Morphology

1. Introduction

Hard water generates adherent deposits of scale on the internal walls of industrial or domestic equipments which cause severe technical problems such as clogging of pipes reduced heat transfer etc. leading to the shutdown of an industrial plant in extreme case [1]. The dissolved minerals get supersaturated and precipitate out because of their inverse solubility and changes in pH of water and get deposited as scale [2]. Depending on the ions present in the water, the composition of the scale varies. Usually barite or sulphides, dominate the scale when barium is present and $CaCO_3$ in the form of calcite and aragonite are some of the major components when calcium is rich in the water [3]. $CaCO_3$ exists in three anhydrous crystalline phases (calcite, aragonite and vaterite) and two hydrated polymorphs (monohydrate and hexahydrate) [4,5]. Under normal conditions, thermodynamically the least stable phase is vaterite while aragonite is metastable and calcite is the most stable [6].

The polymorphism in $CaCO_3$ mainly depends on the precipitation conditions such as pH, temperature, supersaturation levels, presence of additives etc. Water when supersaturated nucleation begins followed by crystal growth. These solid particles either float as suspended particles in the solution or get deposited on the surface as scale. Several factors can influence the formation of scale on metal surfaces. When the surface is heated, the localized higher temperature of the surface boosts the rates of both nucleation and crystal growth which is the thermodynamic driving force scale formation [2]. Literature on crystallization of $CaCO_3$ showed that the nature of the template used and temperature can affect the morphology of crystallized $CaCO_3$ [7].

Scaling can be prevented by physical and chemical techniques. Usage of chelating agents as scale inhibitors is known for decades. The prime effect of a chelating agent is to reduce the supersaturation by complexing with scale causing ions. Many chelating such as ethylenediam-

---

*Corresponding author.

1944-3994 / 1944-3986

minetetraaceticacid (EDTA) [8], NTA [9], HEDP [10], DTPA [11], HEDTA [12] etc. have been studied extensively for their effect on polymorphism in $CaCO_3$. To the best of our knowledge the effect of EGTA on the crystallization of $CaCO_3$ has not been reported. In this paper we report the effect of EGTA on the crystallization of $CaCO_3$ at three different temperatures; 60, 80 and 100°C.

2. Experimental Procedures:

Analytical grade $CaCl_2$, Na_2CO_3, and EGTA were obtained from Hi-media and used as it is. De-mineralized water was used for the preparation of aqueous solutions. Synthesis of $CaCO_3$ was carried out in a similar way described by Gopi et al. [8]. In a typical procedure 50 ml 0.1 M $CaCl_2$ and 20 ml of 0.1 M EGTA were consecutively added in a round bottom flask, connected to a water condenser and heated using a rotamantle to 60°C (±1°C) for 2 h and then 50 ml 0.1 N Na_2CO_3 was added drop wise. The solution and the contents were digested at the same temperature for 24 h. After digestion the sample was filtered, washed with distilled water and then dried at 45°C in an oven. Experiments were carried out in the similar way at 80 and 100°C and also using 30 and 40 ml EGTA. The details of the experimental conditions and the samples prepared are presented in Table 1.

The samples were analyzed for the polymorphic composition by FTIR and XRD methods and the morphological studies were done using SEM and FESEM. FT-IR spectra were taken in the range 500–4000 cm^{-1} using Avatar-330 FTIR and JASCO-5300 FTIR instruments after KBr pelletization. The X-ray diffraction (XRD) patterns were recorded on a Bruker D8 Advanced XRD diffractometer with Cu Ka radiation at $\lambda = 1.5406$ Å. Microscopic morphological images were taken using Philips XL30-ESEM scanning electron microscope (SEM) using a beam voltage of 20 kV and FESEM CARL ZESIS with In lens detectors. The samples were coated with gold prior to imaging.

3. Results and discussion

The crystalline forms of $CaCO_3$ polymorphs were initially identified by FTIR spectroscopy and phase transformations were systematically monitored by powder X-ray diffraction. The characteristic carbonate absorption peaks chosen for the different polymorphs in samples are as follows; in-plane bending (ν_4) mode peaks around 700 and 711 cm^{-1} and 745 cm^{-1} for aragonite, calcite and vaterite respectively; out of plane bending peaks (ν_2 mode) around 856 cm^{-1} for aragonite and at 874 cm^{-1} for both calcite and vaterite; symmetric stretching (ν_1 mode) 1082 cm^{-1} to aragonite and 1087 cm^{-1} to vaterite; asymmetric stretching (ν_3 mode) peaks1475 cm^{-1} and 1450 cm^{-1} for aragonite and vaterite respectively [8,13–15].

FTIR spectra of samples prepared with 20 ml, 30 ml and 40 ml EGTA at 60°C, 80°C and 100°C are presented in Figs. 1–3 respectively. The bands corresponding to aragonite and calcite are highlighted as A and C for respectively. Bands around 700, 856, and 1082 cm^{-1} confirmed the presence of aragonite in all the samples. Presence of bands at 711 and 875 confirmed the existence of calcite also. There was no characteristic band of vaterite at 745 cm^{-1}. This confirmed that all the samples invariably contained a binary mixture of calcite and aragonite.

Confirmation of the phases and quantitative estimation was done by using XRD studies. XRD pattern of samples prepared with 20 ml, 30 ml and 40 ml EGTA are presented in Figs. 4–6 respectively. The percentage of calcite and aragonite present in the samples were calculated using Kontoyannis equation [16] is presented in Table 2.

The observations made in FTIR was ascertained and confirmed in XRD patterns. It is clear from the XRD that all samples contained only calcite and aragonite. From Table 2 it could be observed that with 20 ml EGTA, the molar fraction of aragonite and calcite was found to be 0.21:0.79, 0.28:0.72 and 0.38:0.62 at 60, 80 and 100°C respectively. When the EGTA concentration was increased to 30 ml, the molar fraction became 0.24:0.76, 0.6:0.4 and 0.71:0.29 at 60, 80 and 100°C respectively. Further increase in EGTA (to 40 ml) resulted only lesser amount of aragonite viz 0.66, 0.49 and 0.28 at 60, 80 and 100°C respectively.

It is evident from the data that the amount of aragonite was maximum when 20 ml EGTA was used. Increased usage of EGTA did not favor increase in percentage of aragonite or presence of vaterite in the sample. Similarly increase in temperature could lead to increased percentage of calcite in all the cases. The maximum amount of aragonite was reported at 60°C and with 20 ml EGTA. With increase in temperature, percentage of aragonite is reduced and the amount of calcite increased. The XRD patterns showed good agreement with standard JCPDS card numbers 862339 and 760606 for calcite and aragonite respectively.

According to Ostwald's rule of stages, the transformation usually occur from the least stable polymorph to the most stable polymorph. It is obvious from Figs. 4–6 (a–c) and Table 2 that vaterite is absent at all temperatures. This showed that, the presence of EGTA interacts with the mineral surfaces due to which it could kinetically inhibit the transformation only from aragonite to the thermodynamically most stable polymorph calcite. Nevertheless the transformation from vaterite to aragonite has occurred at ease and even traces of vaterite were not observed in any of the samples even at higher concentration of EGTA. This categorically demonstrates the disability of EGTA to kinetically inhibit the transformation from vaterite to aragonite.

Table 1
Details of samples synthesized in presence of EGTA

S. No	Vol. of EGTA (ml)	Temp. (°C)	Digestion Time h	Initial pH	Final pH
1	20	60	24	8.7	7.1
2	20	80	24	8.7	7.0
3	20	100	24	8.5	7.2
4	30	60	24	8.9	7.4
5	30	80	24	8.6	7.2
6	30	100	24	8.7	7.0
7	40	60	24	8.6	7.1
8	40	80	24	8.4	7.0
9	40	100	24	7.5	6.9

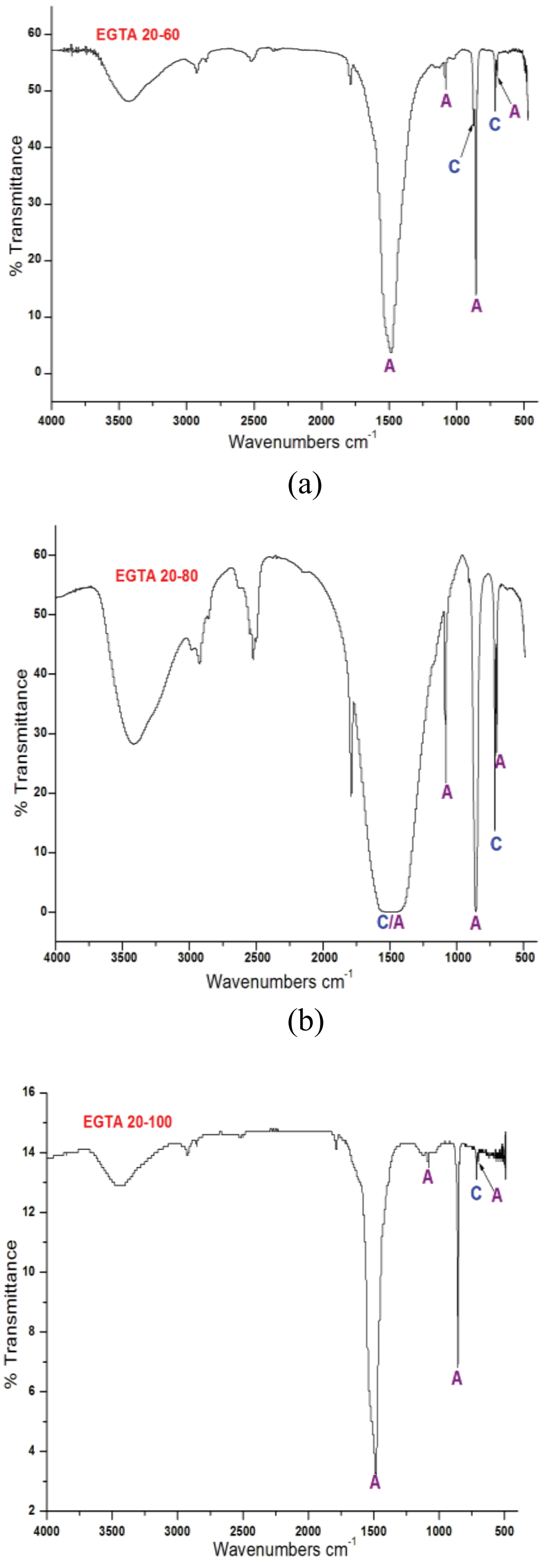

(a)

(b)

(c)

Fig. 1. FTIR spectra of samples prepared with 20 ml EGTA at (a) 60°C (b) 80°C (c) 100°C.

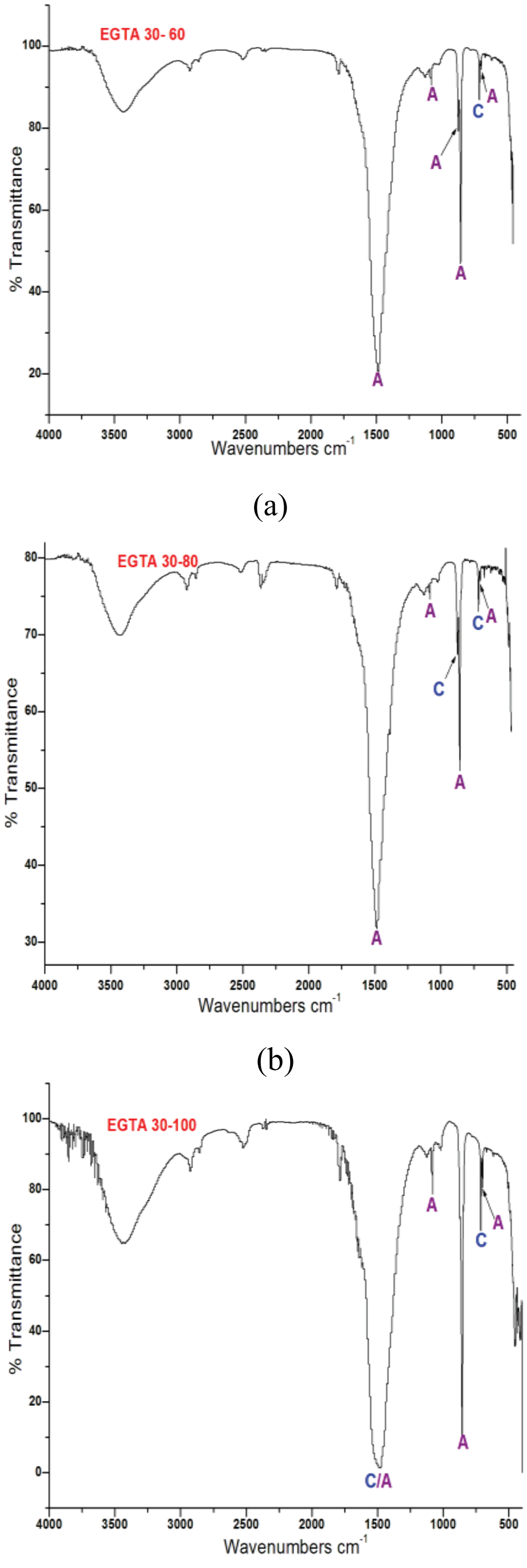

(a)

(b)

(c)

Fig. 2. FTIR spectra of samples prepared with 30 ml EGTA at (a) 60°C (b) 80°C (c) 100°C.

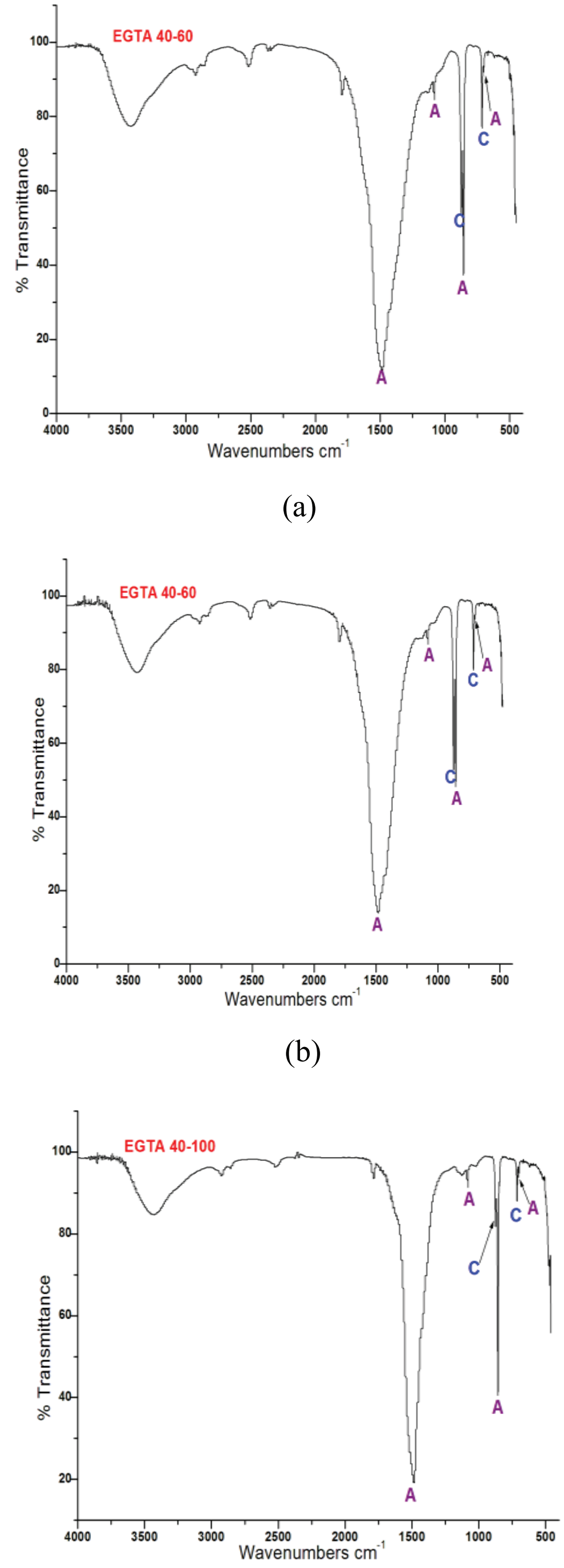

(a)

(b)

(c)

Fig. 3. FTIR spectra of samples prepared with 40 ml EGTA at (a) 60°C (b) 80°C (c) 100°C.

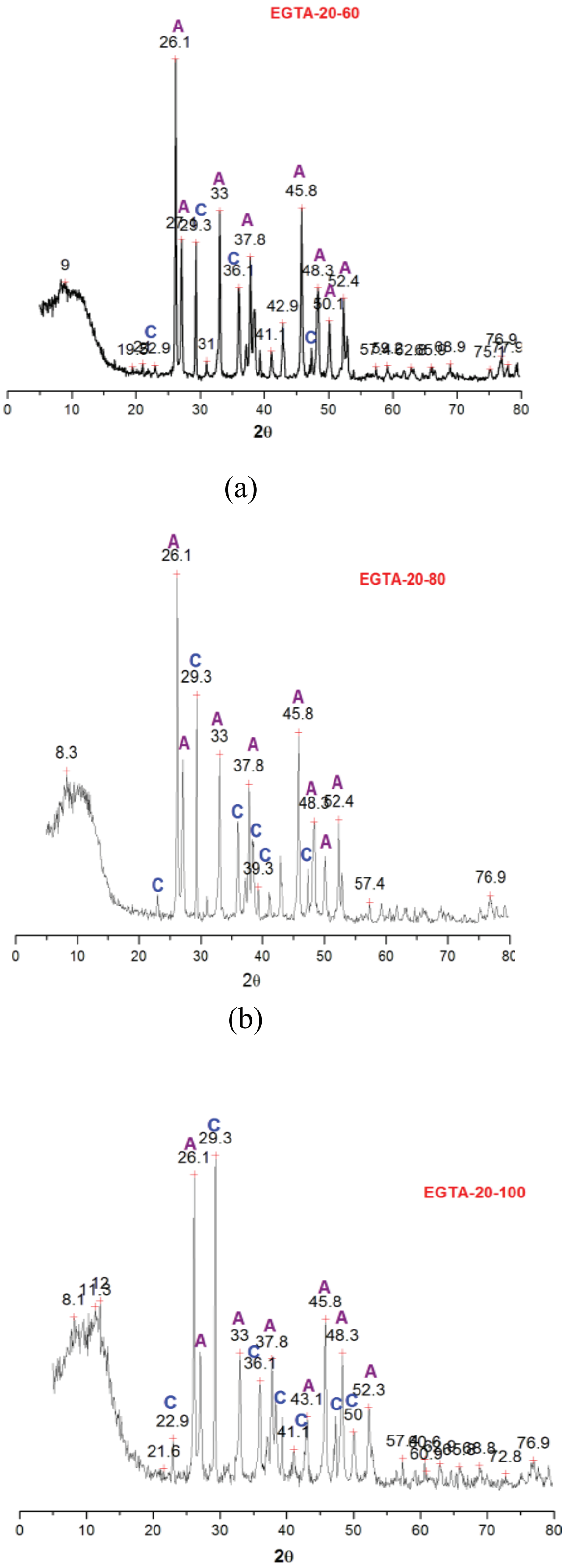

(a)

(b)

(c)

Fig. 4. XRD pattern of samples prepared with 20 ml EGTA at (a) 60°C (b) 80°C (c) 100°C.

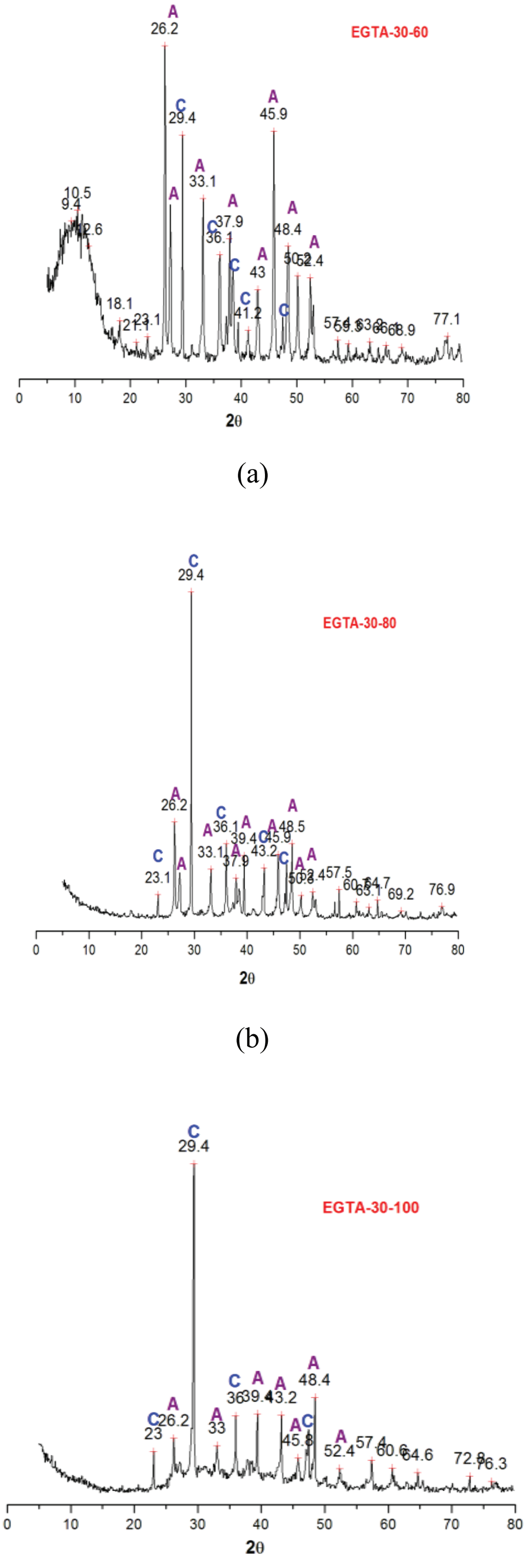

(a)

(b)

(c)

Fig. 5. XRD pattern of samples prepared with 30 ml EGTA at (a) 60°C (b) 80°C (c) 100°C.

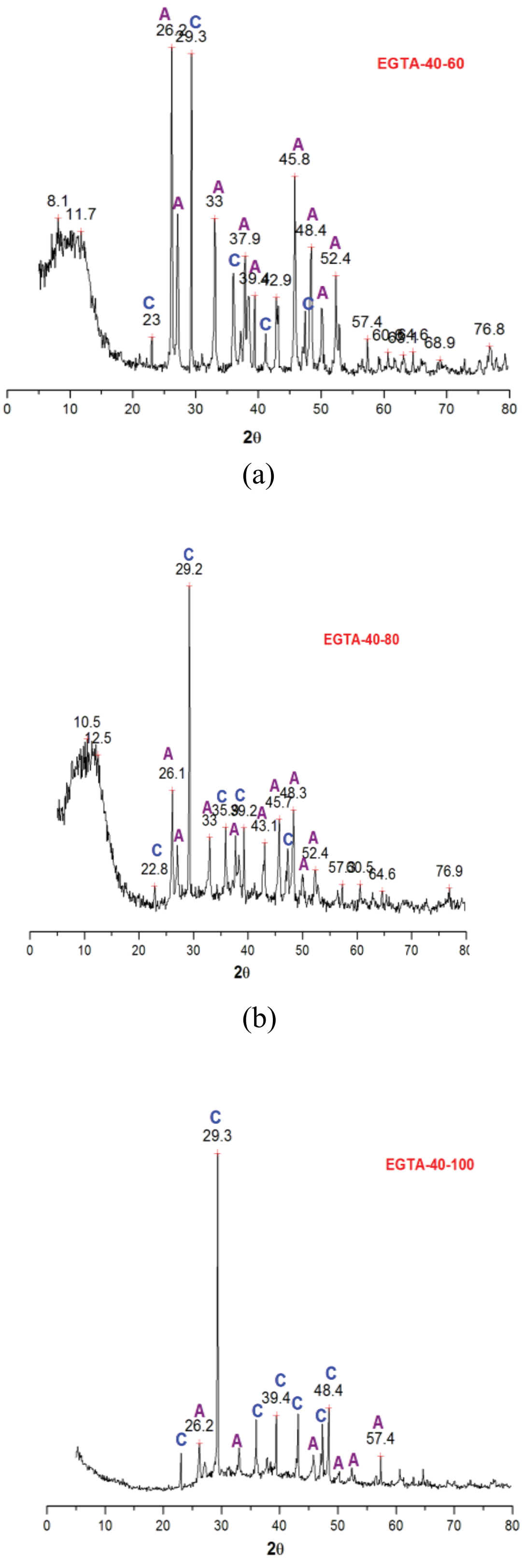

(a)

(b)

(c)

Fig. 6. XRD pattern of samples prepared with 40 ml EGTA at (a) 60°C (b) 80°C (c) 100°C.

Table 2
Percentage composition of different polymorphs of $CaCO_3$

Volume of EGTA ml	Temp (°C)	Percentage of different polymorphs		
		Calcite	Aragonite	Vaterite
20	60	21	79	00
	80	28	72	00
	100	38	62	00
30	60	24	76	00
	80	60	40	00
	100	71	29	00
40	60	34	66	00
	80	51	49	00
	100	72	28	00

The SEM images of sample prepared at 60, 80 and 100°C with 20 ml, 30 ml and 40 ml EGTA are are presented in Figs. 7–9 (a–c) respectively. The morphology of all the samples synthesized with 20 ml EGTA contained two major structures; one containing agglomerated needle like entities resulting datura pods and another thick rod like structures having pointed ends. More or less similar structures were seen with higher concentrations (30 and 40 ml EGTA) also.

The most common morphologies for different polymorphs of $CaCO_3$ are regular rhomboidal, needle/rod and spherical for calcite, aragonite and vaterite respectively [17–19]. It has been reported that in the absence of any additives, needle/rod/flakes like aragonite with rhomboidal calcite are obtained between 60 and 170°C and pure rhomboidal calcite above 170°C [20].

All the SEM images invariably contained ellipsoidal morphology. There was no characteristic rhomboidal morphology pertaining to calcite. The SEM images exhibited more structured morphology with 20 and 30 ml EGTA at 100°C (Fig. 7c and Fig. 8c). As could be seen from the image (Fig. 7c) the datura pod structure formed by the agglomeration of fine micro needle like structures became more spherical.

The XRD and FTIR data elucidated presence of both calcite and aragonite in all samples. None of the SEM images exhibited characteristic rhomboidal morphology of calcite. There are only two structures in most of the SEM images; needle and the Datura pod. The needle structure is the most common structure of aragonite and hence it could not be attributed to calcite. The only structure left out that can be assigned to calcite is the 'datura pod'. The transformation of agglomerated needle like morphology to a more spherical datura pod structure along with increase in calcite mole fraction with increase in temperature, confirmed that this morphology could be attributed to calcite. Needle like morphology is a characteristic morphology of aragonite. Another morphology which was observed at higher concentration of EGTA and could be attributed to calcite is the ellipsoidal structure (Fig. 9a). This structure of calcite could be due to the dissolution of the edges and corners of the usual rhomboidal structure of calcite. Detailed examination of synthesis and characterization of $CaCO_3$ without any additives under

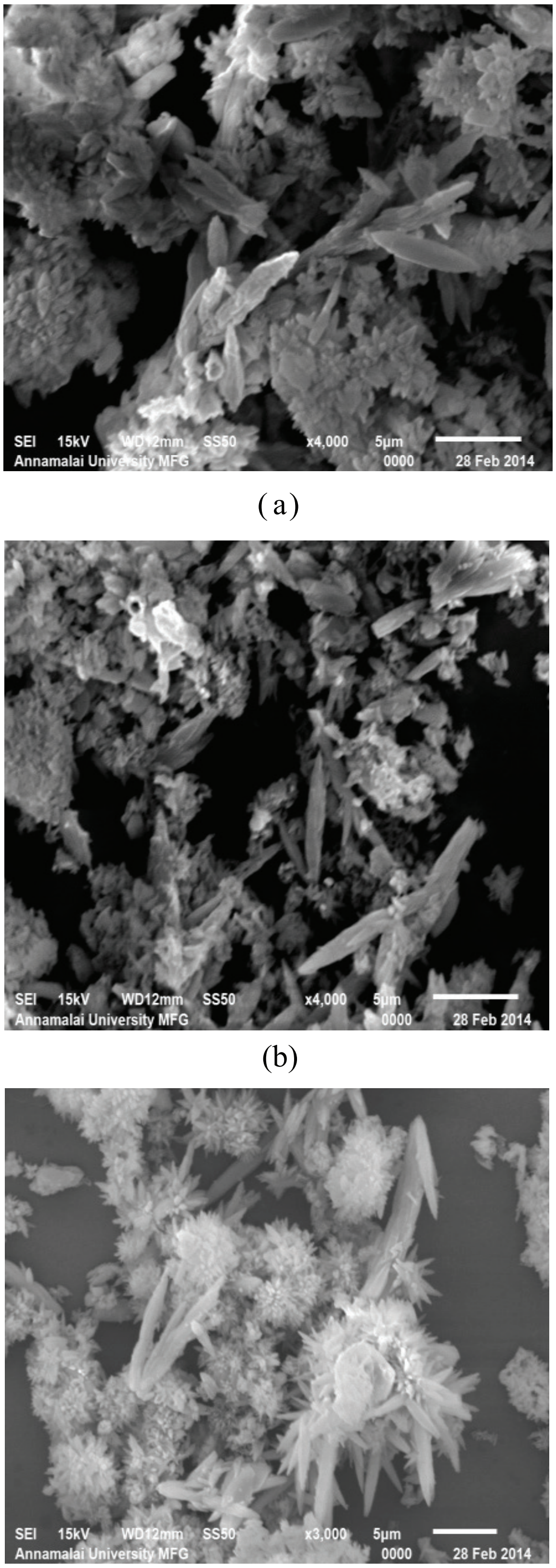

(a)

(b)

(c)

Fig. 7. SEM images of samples prepared with 20 ml EGTA at (a) 60°C (b) 80°C (c) 100°C.

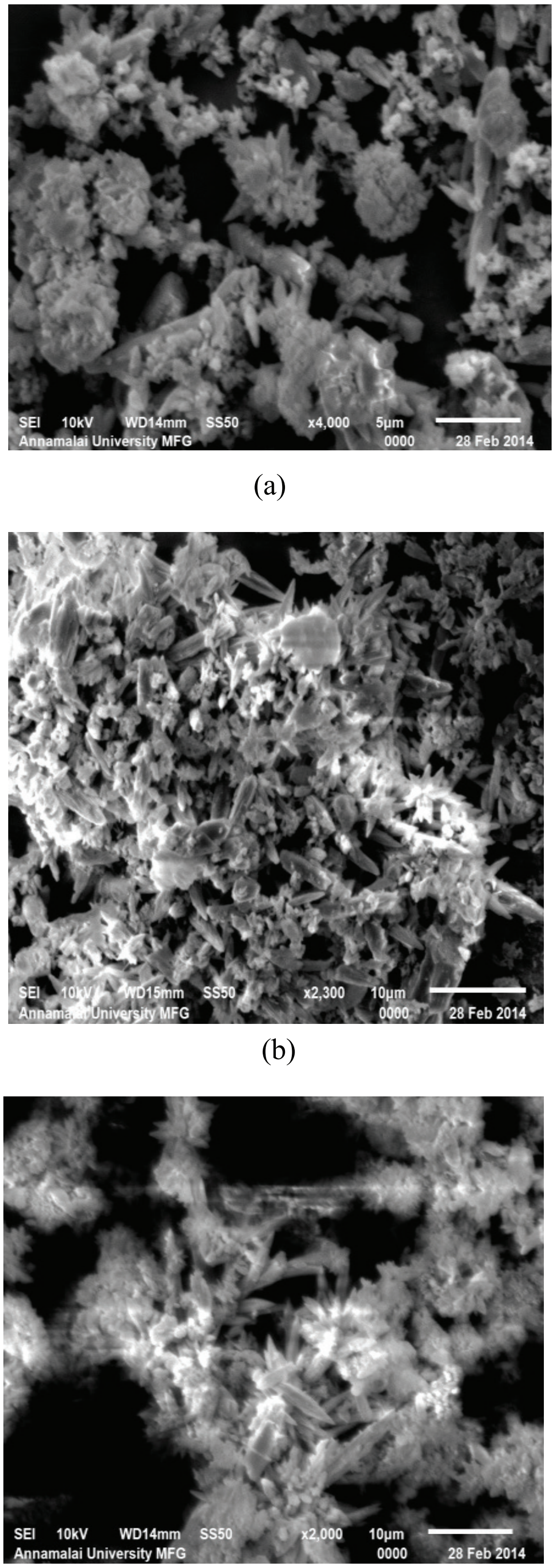

(a)

(b)

(c)

Fig. 8. SEM images of samples prepared with 30 ml EGTA at (a) 60°C (b) 80°C (c) 100°C.

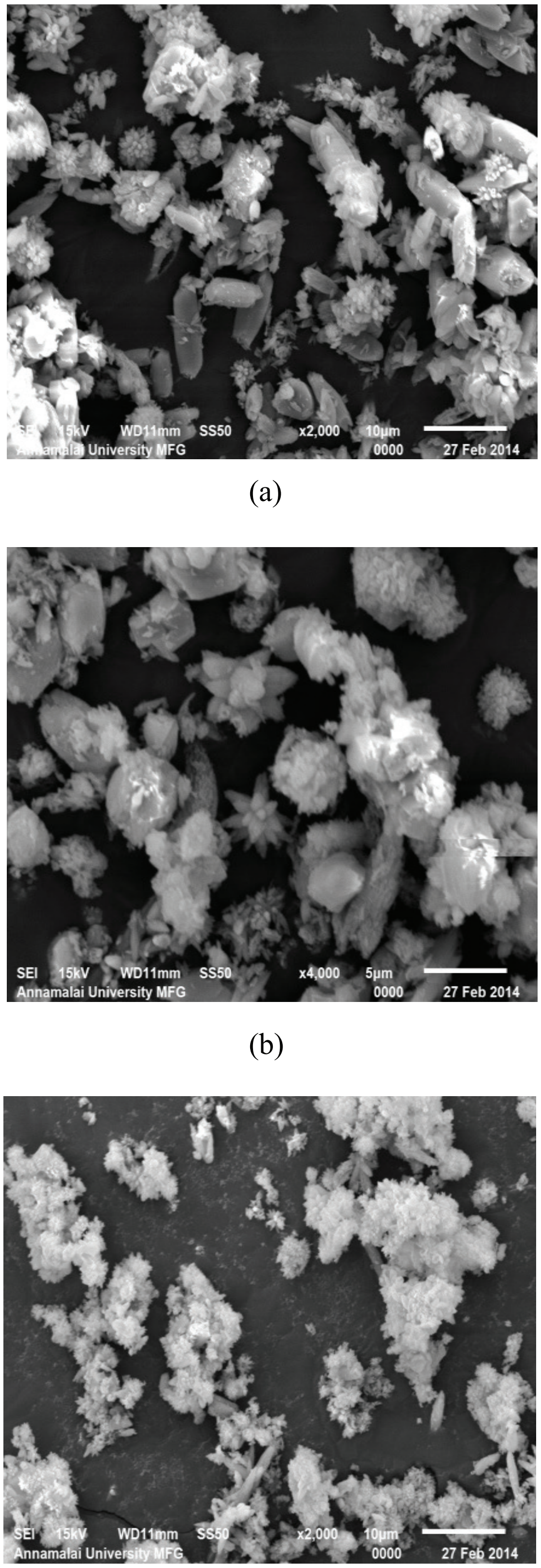

(a)

(b)

(c)

Fig. 9. SEM images of samples prepared with 40 ml EGTA at (a) 60°C (b) 80°C (c) 100°C.

similar conditions have been reported by Gopi et al [8]. Even though absence of any chelating agents stabilized a binary mixture of aragonite calcite below 170°C the morphologies observed were needle and rhombohedral respectively. The datura pod structure of calcite is not reported yet.

It is obvious from the above discussions that EGTA has significant influence on the crystallization process of $CaCO_3$ and has facilitated the crystallization of aragonite. Absence of vaterite in any of the samples even at different concentrations of EGTA and presence of aragonite and calcite in all the samples clearly indicate that the formation of aragonite is a direct crystallization from solution or from amorphous form bypassing the formation of vaterite. The SEM images also never exhibited spherical or any other morphology related to vaterite clearly indicating its absence. Thus, the process of stage conversion the presence of EGTA has enabled the Ostwald's rule of stages to slip the formation of least stable vaterite during the transformation from amorphous to calcite. In some of our earlier studies [10–12] we have observed that crystallization of $CaCO_3$ does not follow the Ostwald's rule of stages at elevated temperatures in the presence of chelating agents.

The possible mechanism of stabilization of aragonite and datura pod like morphology for calcite could be as follows. EGTA is well known for its good chelating ability towards calcium ions. This induces a strong resistance to release Ca^{2+} ions from EGTA-Calcium complex, when Na_2CO_3 is introduced into the system. But as the concentration of CO_3^{2-} exceeds, the ionic product exceeds the solubility product of $CaCO_3$, forcing the EGTA-Ca complex to release the calcium ions to maintain the ionic equilibrium resulting the precipitation of $CaCO_3$. This is obvious from the steady decrease in the pH value after the completion of the reaction time (Table 1). During this process the EGTA is released and is freely available in the reaction environment and they exert resistance to the formation of $CaCO_3$. This results into the dissolution of amorphous and least stable vaterite forms. During digestion, the nucleation and crystal growth occur along with recrystallization favoring aragonite crystals which has the tendency to get converted into calcite. Since the transformation takes place directly from aragonite which usually has the needle like morphology, the agglomeration of needle like structure results into the datura pod like morphology for calcite, rather formation of rhomboidal calcite. Increase in temperature enhances this effect due to the high dissolution and recrystallization rate leading to more structured spherical agglomeration of needle aragonite bundles at 100°C Fig. 9(c). In the absence of scale inhibitors it is reported that [21] metastable phases usually transform into stable phase, and hence calcite becomes the main constitute of scale. When scale inhibitors are added, both formation and transformation of metastable phases are inhibited, which results in the occurrence of aragonite and vaterite. It is observed that the scale largely consist of aragonite at all the temperatures under study indicating that EGTA can be a moderate antiscaling agent.

4. Conclusion

The study revealed a novel datura pod structure for calcite in presence of EGTA. The data indicated that the EGTA influenced the crystallization of $CaCO_3$ by arresting the formation of amorphous and vaterite forms. Increase of temperature helped the formation of more spherical and thorny datura pod structure for calcite. The results demonstrated that aragonite is stabilized more efficiently at 60 °C and with increase in temperature, results into the transformation of calcite. The control over a unique thorny spherical calcite was achieved through this method.

References

[1] Z. Amjad, P.G. Koutsoukos, Evaluation of maleic acid based polymers as scale inhibitors and dispersants for industrial water applications, Desalination, 335 (2014) 55–63.

[2] Z. Wu, J.H. Davidson, L.F. Francis, Effect of water chemistry on calcium carbonate deposition on metal and polymer surfaces, J. Colloid Interface Sci., 343 (2010) 176–187.

[3] M. Yanga, X. Jin, Q. Huang, Facile synthesis of vaterite core-shell microspheres, Colloids and Surfaces, A: Physicochem. Eng. Aspects., 374 (2011) 102–107.

[4] M. Yang Q. Huang, X. Jin, Facile synthesis of the assembled hexagonal vaterite plates and the application as red phosphor doped with Eu^{3+} ions, Colloids and Surfaces A: Physicochem. Eng. Aspects., 386 (2011) 87–91.

[5] X. Yang, G. Xu, The influence of xanthan on the crystallization of calcium carbonate, J. Cryst. Growth., 314 (2011) 231–238.

[6] H. Colfen, Precipitation of carbonates: recent progress in controlled production of complex shapes, Curr. Opin. Colloid Interface Sci., 8 (2003) 23–31.

[7] H. Matahwa, R.D. Sanderson, Surface and statistical analysis of $CaCO_3$ crystals synthesized in the presence of fluorescein-tagged starch grafted with polyacrylic acid, J. Cryst. Growth., 311 (2009) 1136–1146.

[8] S.P. Gopi, V.K. Subramanian, Polymorphism in $CaCO_3$ – Effect of temperature under the influence of EDTA (di sodium salt), Desalination, 297 (2012) 38–47.

[9] S.P. Gopi, K. Palanisamy, V.K. Subramanian, Effect of NTA and temperature on crystal growth and phase transformations of $CaCO_3$, Desal. Water Treat., 54(2) (2015) 316–324.

[10] S.P. Gopi, P. Vijaya, V.K. Subramanian, Morphological and crystallization process of $CaCO_3$ in the presence of Aqua Soft 330 (AS330), Powder Technol., 225 (2012) 58–64.

[11] S.P. Gopi, V.K. Subramanian, K. Palanisamy, Aragonite-calcite-vaterite: A temperature influenced sequential polymorphic transformation of $CaCO_3$ in the presence of DTPA, Mater. Res. Bull., 48 (2013) 1906–1912.

[12] S.P Gopi, V.K. Subramanian, Anomalous transformation of calcite to vaterite: significance of HEDTA on crystallization behavior and polymorphism at elevated temperatures, Indian J. Chem., Sect. A., 52 (2013) 342–349.

[13] F.A. Andersen, L.J. Brecevic, Infrared spectra of amorphous and crystalline calcium carbonate, Acta Chem. Scand., 45 (1991) 1018–1024.

[14] N.V. Vagenas, A. Gatsouli, C.G. Kontoyannis, Quantitative analysis of synthetic calcium carbonate polymorphs using FT-IR spectroscopy, Talanta, 59 (2003) 831–836.

[15] S.F. Chen, S.H. Yu, J. Jiang, F.Q. Li, Y.K. Liu, Polymorph discrimination of $CaCO_3$ mineral in an ethanol/water solution: formation of complex vaterite superstructures and aragonite rods, Chem. Mater., 18 (2006) 115–122.

[16] C.G. Kontoyannis, N.V. Vagenas, Calcium carbonate phase analysis using XRD and FT-Raman spectroscopy, Analyst, 125 (2000) 251–255.

[17] C. Li, G.D. Botsaris, D.L. Kaplan, Selective in vitro effect of peptides on calcium carbonate crystallization, Cryst. Growth Des., 2 (2002) 387–393.

[18] N. Andritsos, A.J. Karabelas, P.G. Koutsoukos, Morphology and structure of $CaCO_3$ scale layers formed under isothermal flow conditions, Langmuir, 13 (1997) 2873–2879.

[19] I. Udrea, C. Capat, E.A. Olaru, R. Isopescu, M. Mihai, C.D. Mateescu, C. Bradu, Vaterite synthesis via gas−liquid route under controlled pH conditions, Ind. Eng. Chem. Res., 51 (2012) 8185−8193.

[20] J.H. Guo, S.J. Severtson, Application of classical nucleation theory to characterize the influence of carboxylate-containing additives on $CaCO_3$ nucleation at high temperature, pH, and ionic strength, Ind. Eng. Chem. Res., 42 (2003) 3480–3486.

[21] G.C. Zhang, J.J. Ge, M.Q. Sun, B.L. Pan, T. Mao, Z.Z. Song, Investigation of scale inhibition mechanisms based on the effect of scale inhibitor on calcium carbonate crystal forms, Sci. China B Chem., 50 (2007) 114–120.